

Modeling of Feedback and Rotation Stabilization of the Resistive Wall Mode in Tokamaks

**by
M.S. Chu**

**for V.S. Chan, M.S. Chance,* D.H. Edgell,‡ A.M. Garofalo,Δ A.H. Glasser,†
S.C. Guo,# D.A. Humphreys, T.H. Jensen, J.S. Kim,‡ R.J. La Haye,
L.L. Lao, G.A. Navratil,Δ M. Okabayashi,* F.W. Perkins, H. Reimerdes,Δ
H.E. St. John, E. Soon,§ E.J. Strait, A.D. Turnbull, M.L. Walker, and S.K. Wong**

***Princeton Plasma Physics Laboratory, Princeton, New Jersey.**

†Los Alamos National Laboratory, Los Alamos, New Mexico.

‡ FARTECH, Inc., San Diego, California.

ΔColumbia University, New York, New York.

#Consorzio RFX, Padova, Italy.

§University of California - San Diego, La Jolla, California.

**Presented at
19th IAEA Fusion Energy Conference
Lyon, France**

October 14–19, 2002



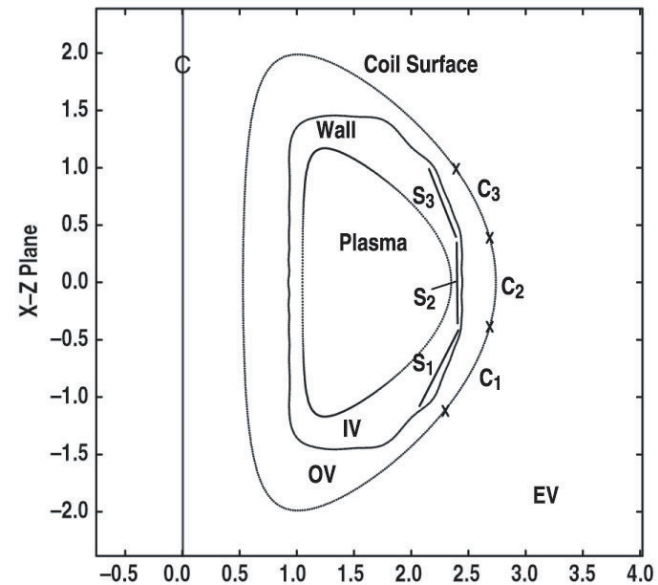
270-02/MS/JY

MOTIVATION

- The goal of the advanced tokamak reactor aims to design an attractive fusion reactor which operates in steady state at high fusion power density by simultaneously maximizing the plasma β , the energy confinement time and the fraction of non inductive bootstrap current
- The β limit in advanced tokamak designs are invariably set by low toroidal mode number external kink MHD modes
- The external kinks can be stabilized by placing a perfectly conducting shell sufficiently close to the edge of the plasma. This external conducting shell is essential for achieving acceptable β in the advanced tokamak reactor
- However, the stabilizing external shell possesses a small but finite resistivity. This converts the external kink mode into a slowly growing MHD mode - the resistive wall mode, (RWM) which can destroy the plasma
- The RWM can be stabilized either by plasma rotation and dissipation or by active feedback

NORMAL MODE FORMULATION FOR GENERAL GEOMETRY

- A formulation is presented for the feedback stabilization of the RWM
 1. General static plasma equilibrium, i.e. helical or axisymmetric plasma
 2. General external modes. i.e. helical external kink or vertical displacements
 3. A Non-self-adjoint energy functional



$$\delta W_p + \delta K + \delta W_v + D_W + \delta E_C = 0$$

(1)

- The full solution of the problem consists of three steps:
 1. Open loop stability $\delta E_C = 0$. Generalization of the ideal MHD stability problem
 2. Formation of excitation and sensor matrices of the feedback coils and sensor loops
 3. -SISO: Nyquist study of the stability with feedback
-MIMO: Solution of the characteristic equations of the closed loop feedback system

THE OPEN LOOP STABILITY AND OPEN LOOP EIGENFUNCTIONS

- Without the external coils, the energy expression is self-adjoint: a generalization of ideal MHD and diagonalizable by a set of orthonormal eigenfunctions with discrete eigenvalues

$$\delta W_p(i, j) + \delta W_v(i, j) + \frac{1}{2} \gamma_i \delta_{i,j} = 0 \quad (2)$$

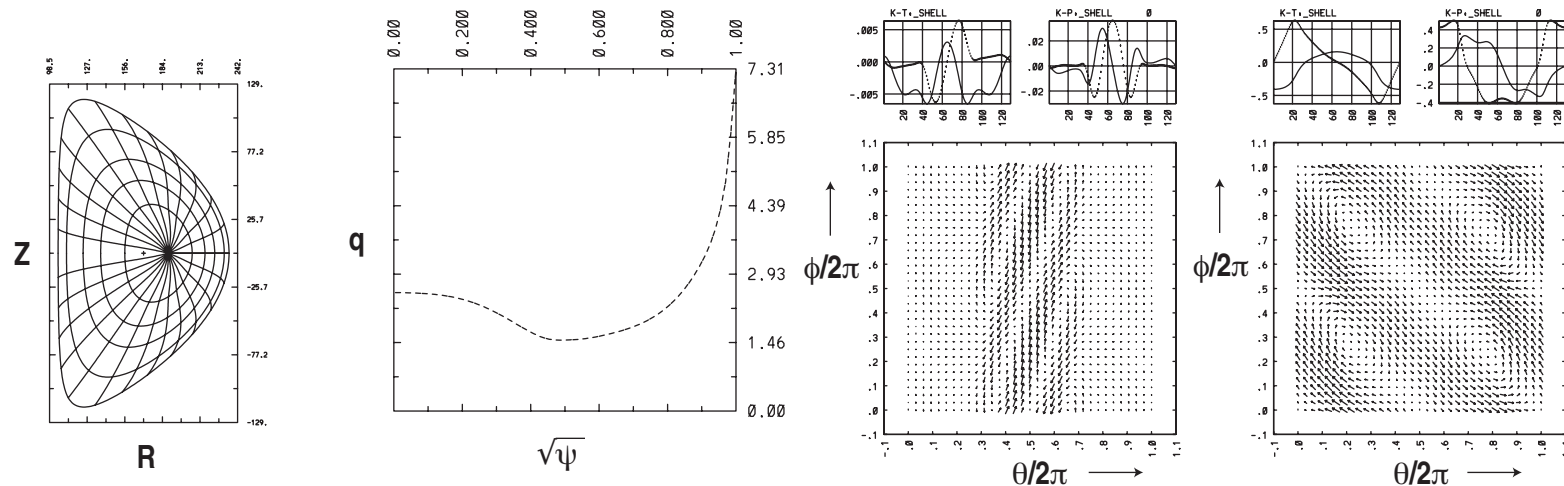


Figure 1: The equilibrium flux plot, the q profile and the skin currents on the resistive wall for the first two modes induced by the open loop eigenfunction. For the skin current plots, top left is $n = 1$ Fourier amplitude of poloidal skin current; top right is the Fourier amplitude of toroidal skin current. Bottom is vector plot of skin current in the $\theta - \phi$ plane

DYNAMICS AND CHARACTERISTIC EQUATIONS FOR CLOSED LOOP FEEDBACK

- Utilizing the open loop eigenfunctions, the dynamics of the system is specified completely by

$$\frac{\partial \alpha_i}{\partial t} - \gamma_i \alpha_i = \sum_c I_c E_i^c \quad (3)$$

$$\frac{\partial I_c}{\partial t} + \frac{1}{\tau_c} I_c = \sum_l G_c^l F_l^c (\{\alpha_i\}, \{I_c\}) \quad (4)$$

- The dynamical variables of the system is reduced to $\{\alpha_i, I_c\}$ α_i is the amplitude of the open loop eigenfunction; E_i^c is the excitation matrix; G_c^l is the amplification matrix; and F_l^c is the sensor matrix. The characteristic equation is given by

$$D(s) = \begin{vmatrix} s\vec{I} - \vec{\Gamma} & -\vec{E} \\ -\vec{GF} & s\vec{I} - \vec{L} \end{vmatrix} \quad (5)$$

- Here \vec{I} is the identity matrix; $\Gamma_{ij} = \gamma_i \delta_{ij}$ is the diagonal growth rate matrix; and \vec{L} the coupling matrix of the feedback coils and the direct coupling between the coils and sensors

FEEDBACK WITH SISO: NYQUIST STUDY OF TRANSFER FUNCTION $P(\omega)$

- Feedback with poloidal sensors is superior

$$P(\omega) \equiv \sum_i \frac{F_i E_i}{j\omega - \gamma_i} = \sum_i \frac{R_i}{j\omega - \gamma_i} \quad (6)$$

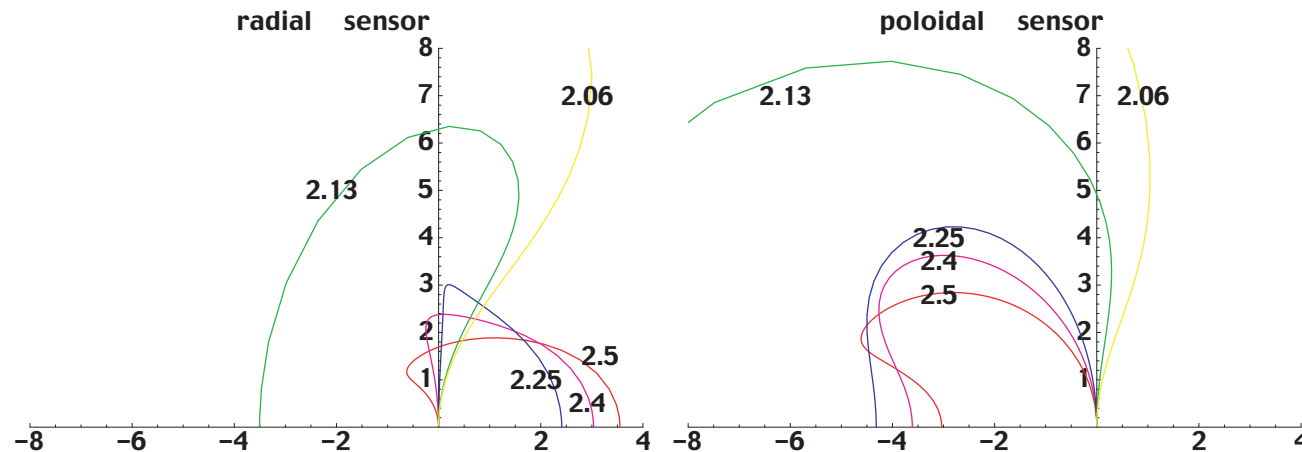
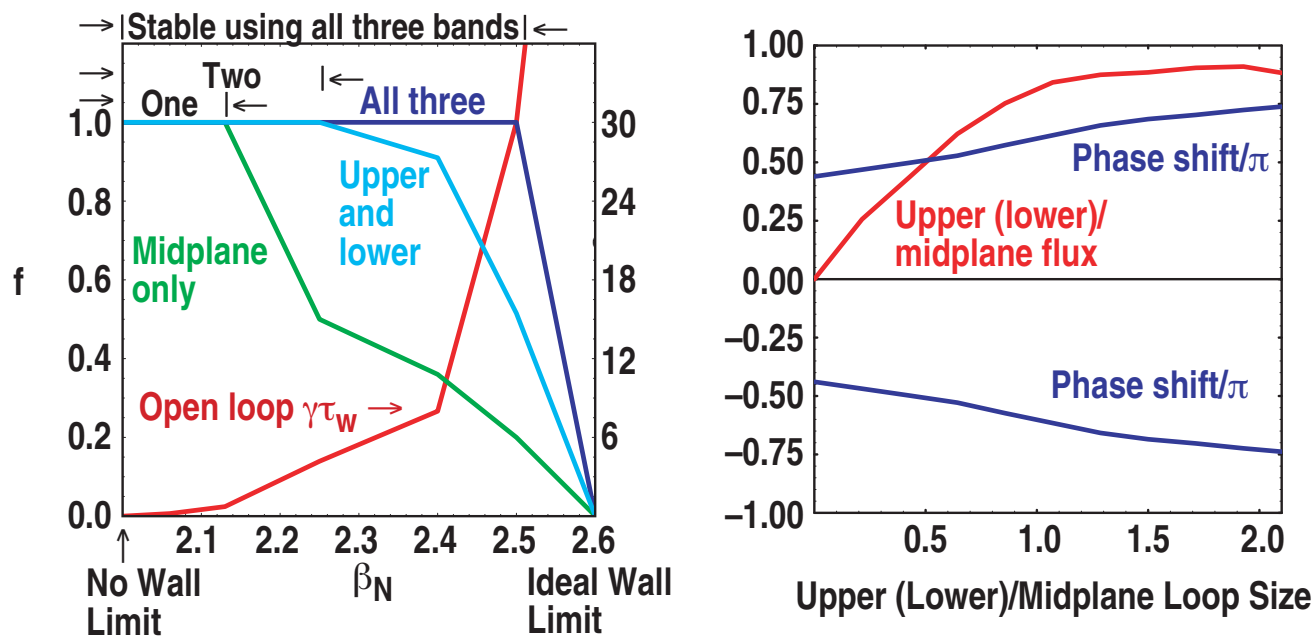


Figure: 2 Nyquist diagrams of transfer functions (ratio of flux detected by the sensor loop to current in the feedback coil) for equilibria with $\beta_n = (2.06, 2.13, 2.25, 2.4, 2.5)$. The curves are symmetric with respect to the horizontal axis. Only the upper half of the curves are shown. On the left is for radial field sensors. The curves labeled 2.06 and 2.13 encircle $(-1, 0)$, showing that at these lower values of β_n s the RWM is stabilized. Equilibria at higher β_n values are not stabilized. On the right is for poloidal field sensors. The RWM is stabilized at all β_n s. Showing that feedback with poloidal sensor is better than with radial sensor.

FEEDBACK WITH MIMO: SOLUTION OF THE CHARACTERISTIC EQUATIONS

SUMMARY OF RESULTS FOR THE DIII-D EQUILIBRIA

WITH DIFFERENT β_N 's AND RADIAL SENSORS



- Left is the growth rate and feedback requirements of the RWM as a function of β_N . Red is the growth rate. The green and blue curves are the filtering factors of the sidebands that are required to stabilize the RWM. With three segments of coils feedback stabilization is feasible for equilibria with $\gamma\tau_w$ up to 30 (with upper and lower segment size equal to that of the midplane.) Right is the flux ratio and ratio and phase angle difference due to the RWM on the upper (lower) and the midplane coil segments as a function of the size of the coils.

GENERAL FORMULATION INCLUDING PLASMA ROTATION AND DISSIPATION

- The “resistive wall mode” can be described in terms of circuits on the resistive wall driven by the plasma or the external coils

$$\frac{\mu_0 \Delta z}{\eta \lambda_{l'_w}} \frac{\partial B_{l'_w}}{\partial t} + \sum_{l_w} M_{l'_w l_w} B_{l_w}^w = \sum_{l_p} C_{l'_w l_p}^{wp} B_{l_p}^p - \sum_{l_c} C_{l'_w l_c}^{wc} I_{l_c} \quad (7)$$

- The plasma responds to the magnetic field $B_{l_w}^w$ on the resistive wall through the relationship

$$B_{l_p}^p = -\frac{1}{\delta W_{Iw} + i\Omega D} C_{l'_p l_w}^{pw} B_{l_w}^w \quad (8)$$

- The response of the RWM to the coil currents is therefore

$$\frac{\mu_0 \Delta z}{\eta \lambda_{l'_w}} \frac{\partial B_{l'_w}}{\partial t} + \sum_{l_w} (M_{l'_w l_w} + \sum_{l_p} C_{l'_w l_p}^{wp} \sum_{l'_p} \frac{1}{(\delta W_{Iw} + iD\Omega)_{l_p l'_p}} C_{l'_p l_w}^{pw}) B_{l_w}^w = - \sum_{l_c} C_{l'_w l_c}^{wc} I_{l_c} \quad (9)$$

THE LUMPED PARAMETER MODEL AND RFA

- For the least stable resistive wall mode and assuming the matrix elements of the energy and dissipation factors are constants, we arrive at a “lumped parameter equation”

$$\tau_w \frac{\partial B_w}{\partial t} + M \frac{1}{A} B_w = C^{wc} I_c \quad (10)$$

- where A is the 'complex amplification factor'. Note that A = 1 in the absence of plasma

$$A = \frac{\delta W_{Iw} + i\Omega D}{\delta W_{nw} + i\Omega D} \quad (11)$$

- In this equation we see that the dissipation on the wall and the dissipation in the plasma are separated

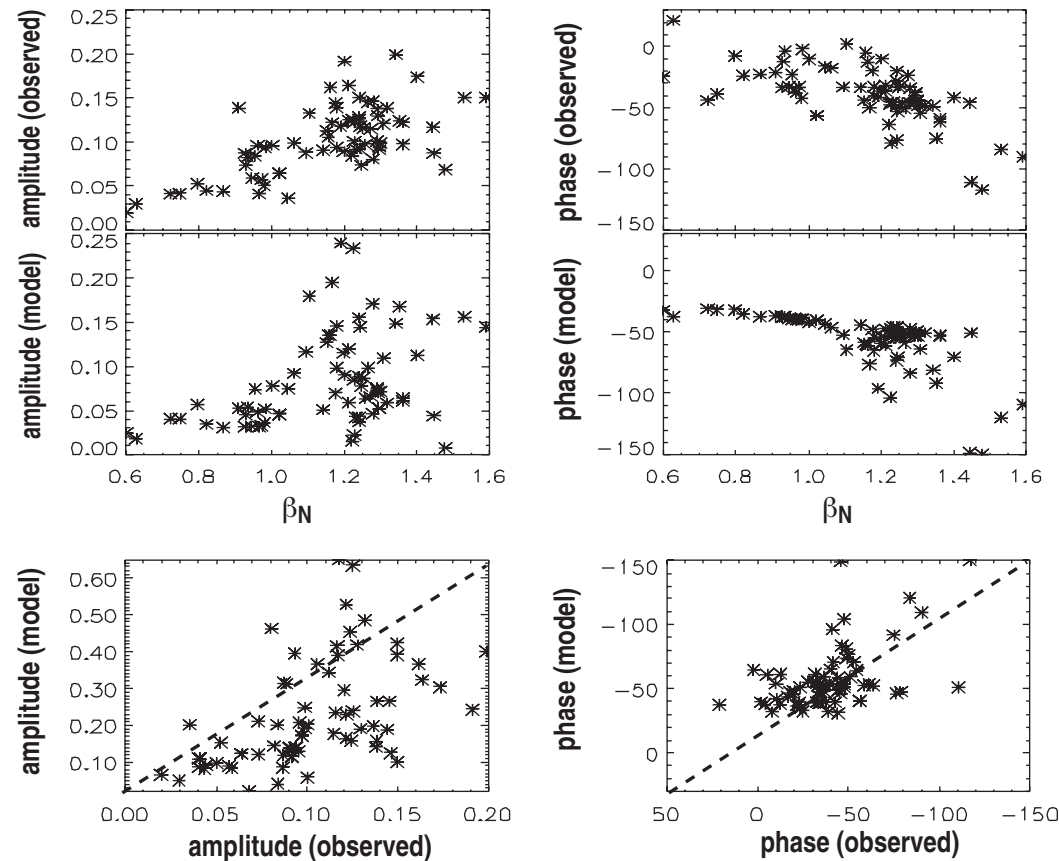
1. 'No External Coil': homogeneous equation, dissipation in plasma and the resistive wall

$$\gamma \tau_w = -M \frac{1}{A} \quad (12)$$

2. 'Steady State with External Coil': inhomogeneous equation. dissipation in plasma

$$B_w = \frac{A}{M} C^{wc} I_c \quad (13)$$

COMPARISON OF LUMPED PARAMETER MODEL WITH EXPERIMENT



$$A = \frac{\delta W_{Iw} + \alpha \Omega^2 + iD\Omega}{\delta W_{nw} + \alpha \Omega^2 + iD\Omega} \quad (14)$$

- Qualitative agreement is also obtained by using the presnet lumped parameter model with different forms for A. This indicates more details should be included in future comparisons

NONUNIFORM ROTATION OF THE RESISTIVE WALL CAN STABILIZE THE RWM

- Growth of the RWM is due to the 'coherent' diffusion of the perturbed magnetic flux of the 'unstable mode' through the resistive wall
- Nonuniform rotation of the resistive wall can destroy the coherency of the perturbed flux which diffuses through the resistive wall and lose its mode structure
- The flow speed required is very modest and varies inversely with τ_w the resistive wall time constant
- This problem was studied semi-analytically by Taylor et al. [Phys. Plasmas, Vol. 8, 4062 (2001)]. The present study utilizes the Mars code by modifying the equation for the flux diffusion through the resistive wall as

$$\frac{\partial \delta B_n}{\partial t} + in\Omega(l_w)\delta B_n = \hat{n} \cdot \nabla \times \delta B \quad (15)$$

REQUIRED ROTATION SPEED IS MODEST AND VARIES INVERSELY WITH τ_w

$$R/a = 3., \kappa = 1.6, q_0 = 1.2\%, q_e = 2.55, \beta = 6.7\%,$$

$$\beta_N = 4.25, \Omega(l_w) = \Omega_0 \cos(l_w), r_{wall} = 1.125r_p, \nu = 0.055$$

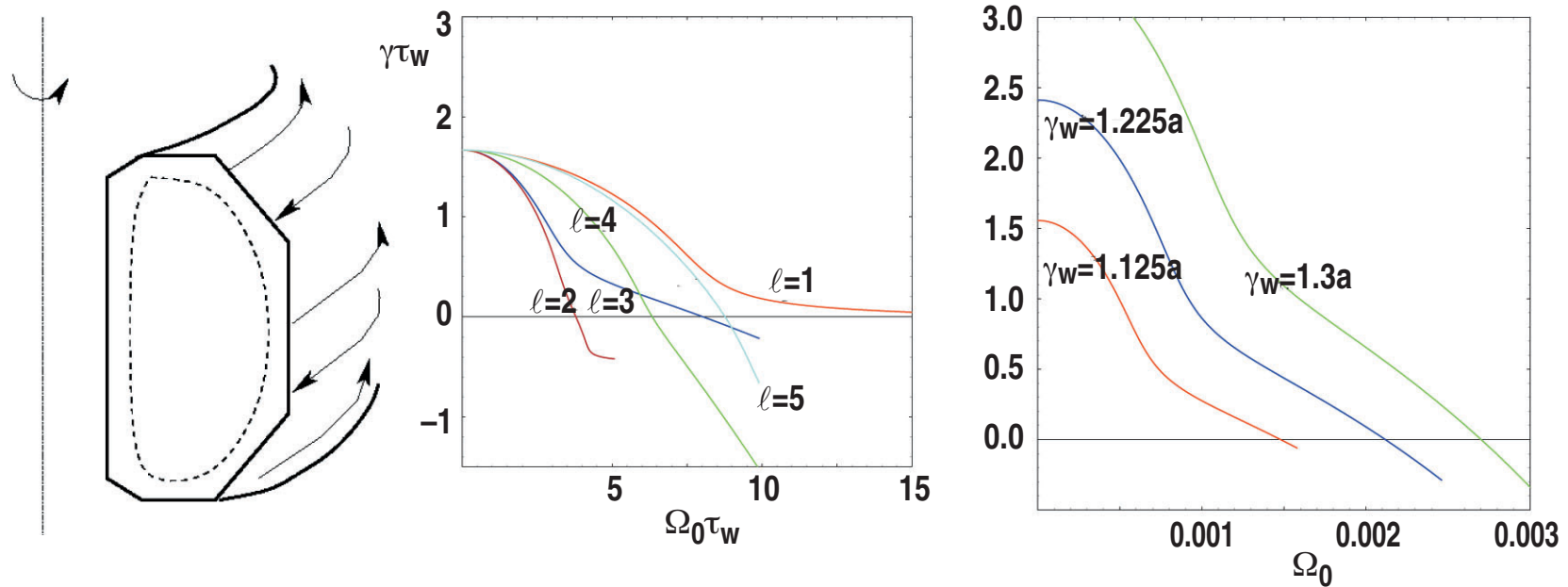


Figure 3: Schematic of the rotation on the resistive wall, growth rates of the RWM with a toroidal flow speed of $\Omega_0 \cos (2\pi\ell l_w/L_w)$ on the resistive wall and the growth rates at three different wall distances. Due to the toroidal nature of the instability, the poloidal harmonics are coupled. A number of different flow patterns with different ℓ numbers are effective. This is further facilitated by plasma viscosity

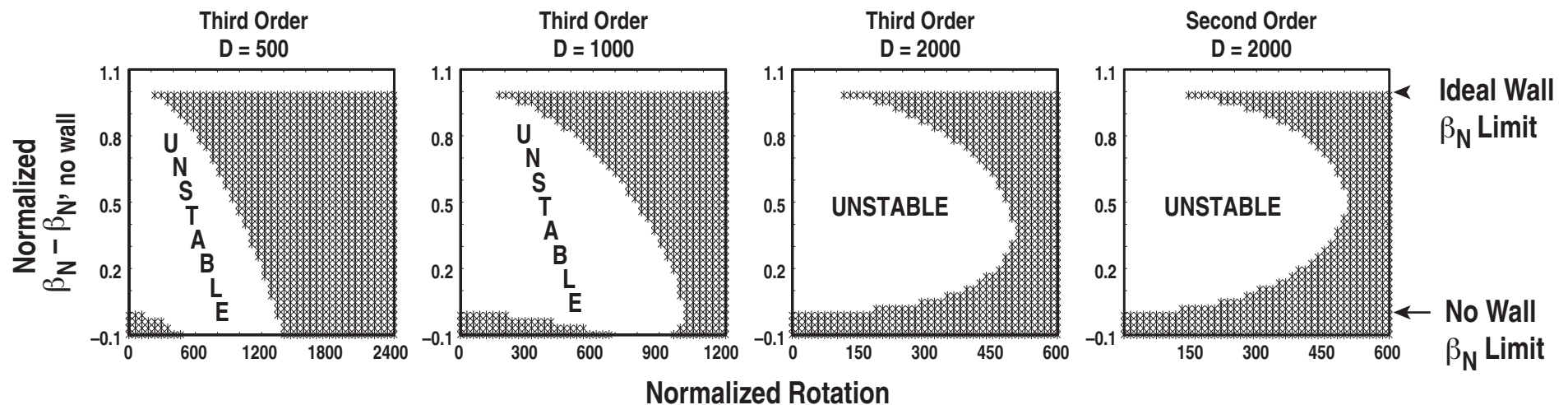
PREDICTIONS OF STABILITY BASED ON STRENGTH OF DISSIPATION

- A general model [M.S. Chu, et al, Phys. Plasmas, 1995] valid for slab, cylinder, torus

$$(\gamma + i n \omega)^2 K + (\gamma + i n \omega) \overset{\text{Dissipation}}{D} + \overset{\text{Plasma Potential Energy}}{\delta W_p} + \frac{\delta W_V^b \gamma \tau_w + \delta W_V^\infty}{\gamma \tau_w + 1} = 0$$

← Plasma Rotation ← D

- ★ Plasma rotation ω and dissipation D can stabilize the RWM ($\text{Re } \gamma < 0$)
for $\beta_N, \text{ no wall} < \beta_N < \beta_N, \text{ ideal wall}$



- ★ For high dissipation, $\omega_{\text{crit}} \approx (-\gamma_{\text{no wall}} * \gamma_{\text{ideal wall}})^{1/2}$
- ↑ Assumed Unstable ↑ Assumed Stable

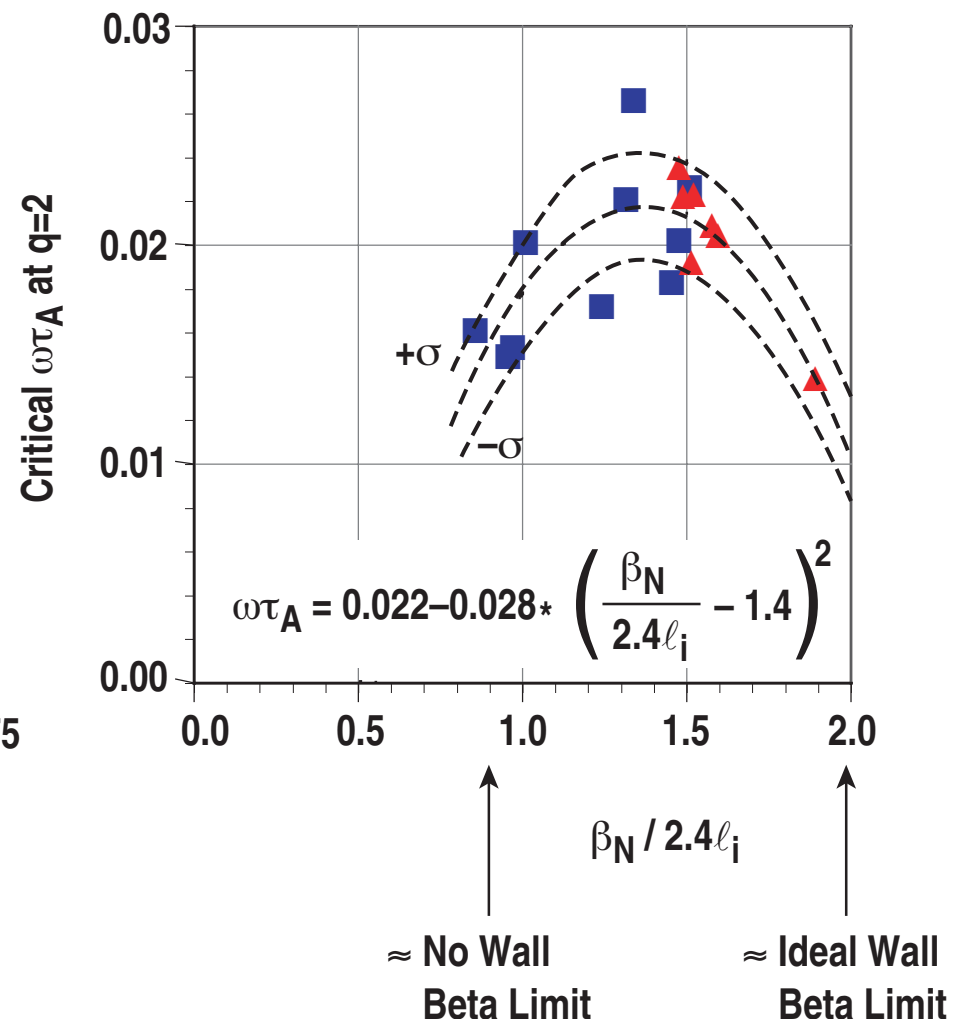
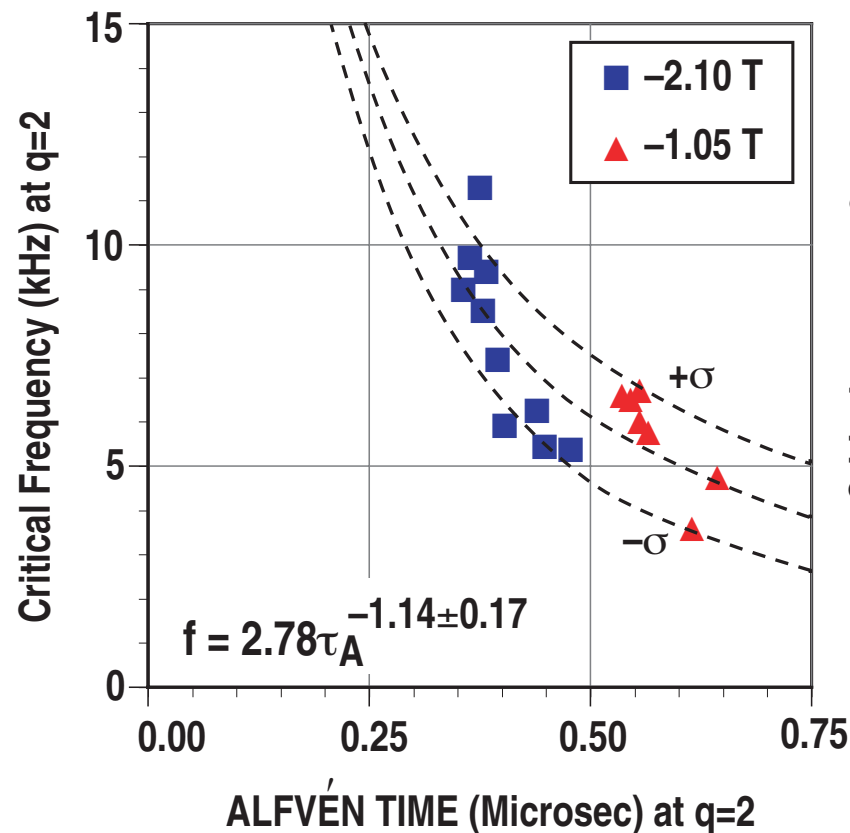
COMPARISON OF STABILITY MODELS WITH EXPERIMENTAL DATA FOR CRITICAL ROTATION FOR ONSET OF $n=1$ RESISTIVE WALL MODE

- Scales as inverse of ALFVÉN TIME

★ “Hidden variable” is $\beta_N / \beta_{N,\text{no wall}}$

... $\beta_N / 2.4\ell_i = 0.9 \sim 1.9$

- Consistent with “high dissipation” dispersion relation



POSSIBILITY OF ROTATIONAL STABILIZATION OF RWM IN ITER-FEAT

$$q_{min} = 2.1, q_{95} = 7.11, \beta = 3.3\%, \beta_N = 3.22, B_0 = 5.3T,$$

$$I_p = 10.1MA, R = 6.34m, a = 1.87m, r_{ideal}/r_{plasma} = 1.5$$

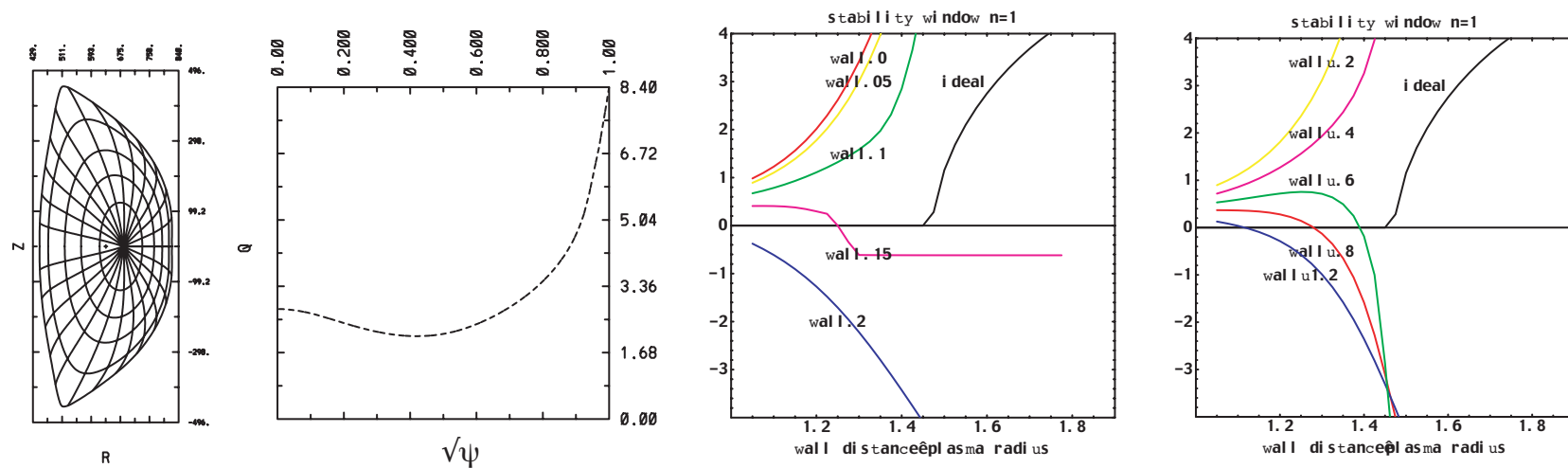


Figure 4: Equilibrium flux plot, q profile and stability windows for the RWM for a possible ITER-FEAT equilibrium. The third panel is the stability window with profiled rotation. The curves are labeled with rotation speed of the plasma center in units of the toroidal Alfvén transit frequency. The fourth panel is labeled by the rotation frequency of the rigid plasma rotation measured in percentage of the toroidal Alfvén transit frequency

CONCLUSION

- Normal mode approach to feedback stabilization of the RWM for a general static plasma equilibrium has been formulated and implemented numerically for the tokamak. Results indicate that feedback using poloidal sensors is superior to using radial sensors
- A general formulation of feedback stabilization of the RWM including plasma rotation and dissipation has been presented. Relationship to the lumped parameter model for the comparison with the resonant field amplification experiment discussed
- Stabilization of the RWM by a nonuniformly rotating resistive wall with very modest rotation speed has been demonstrated numerically
- Further comparison of the lumped parameter stability models for the RWM with the critical rotation speed experiment discussed
- Possibility of rotational stabilization of the RWM in ITER-FEAT demonstrated numerically